

Supplementary Information

Electrostatically Regulated Photoinduced Electron Transfer in “Cationic” Eco-friendly CuInS₂/ZnS Quantum Dots in Water

Jewel Ann Maria Xavier,^{†a} Gayathri Devatha,^{†a} Soumendu Roy,^a Anish Rao^a and
Pramod P. Pillai^{a*}

^aDepartment of Chemistry and Centre for Energy Sciences, India Institute of Science
Education and Research (IISER), Dr. Homi Bhabha Road, Pune, India - 411008.

[†]These authors contributed equally

*Correspondence to: pramod.pillai@iiserpune.ac.in

Section 1: Experimental details and methods:

Materials and Methods: Indium acetate (In(Ac)₃), Copper acetate (Cu(Ac)₂), 1-Dodecanethiol (DDT), 1-Octadecene (ODE), Oleic acid (OA), Zinc stearate (Zn(St)₂), Oleylamine (OAm), Tetramethylammonium hydroxide (TMAOH) 25 % wt. in water, Mercaptoundecanoic acid (MUA), Indocyanine green (ICG) and Methylene Blue (MB) were purchased from Sigma-Aldrich and were used without further purification. N,N,N-trimethyl(11-mercaptopundecyl)ammonium chloride (TMA) was synthesized using a reported procedure.¹

Synthesis of CIS/ZnS QDs: CuInS₂/ZnS core/shell quantum dots were synthesized following a reported protocol.² Briefly, In(Ac)₃ (0.2 mmol, ~58mg) and Cu(Ac)₂ (0.2 mmol, ~36 mg) were mixed with DDT (8.35 mmol, 2 mL), 0.3 mL OA and 3 mL ODE in a 50mL three-neck RB and gently stirred under N₂ atmosphere. The reaction mixture was heated at 100 °C for 10 min until a clear solution was obtained. Subsequently, vacuum was applied for 30 min and the reaction temperature was raised to 230 °C to allow the growth of CIS QDs for 15 min. With the increase in temperature, the reaction solution changed color from light

yellow to yellow to red and finally dark red, indicating nucleation and formation of CIS QDs. The reaction was quenched by lowering the temperature to 50 °C using a water bath. For in-situ ZnS overcoating, a solution of ODE and OAm (4:1 ratio, 1.6 mL and 0.4 mL respectively) containing Zn(St)₂ (0.2 mmol, ~125 mg) was added dropwise to the reaction mixture at 230 °C under N₂ flow over a period of 30 min. Subsequently, the reaction temperature was maintained at 230 °C for about 30 min to allow for shell growth. The reaction was quenched by lowering the temperature to 50 °C, and the resultant QDs were purified by precipitating with ethanol and redispersing in chloroform. This step was repeated three times, and purified CIS/ZnS core-shell QDs were dispersed in chloroform for further studies.

Preparation of water soluble [+] CIS/ZnS QDs: Water soluble [+] CIS/ZnS QDs were prepared via a phase exchange reaction. To a solution containing cationic TMA ligand (~0.2 mmol) dissolved in 2 mL of water, OAm capped CIS/ZnS QDs in chloroform (1 μM, 5 mL) was added and stirred for ~4 h. The progress of the phase transfer reaction can be easily monitored by observing the color changes in the lower organic (dark red to colorless) and upper aqueous (colorless to dark red) phases. The TMA ligand aided in surface functionalization (via the thiol group) as well as in phase transfer (via the quaternary ammonium group) imparting cationic surface charge to the QDs. The aqueous layer was carefully removed and precipitated using isopropanol to remove excess TMA ligands. Finally, the precipitates were redispersed in deionized water, yielding [+] CIS/ZnS QDs. A similar procedure was adapted for preparing [-] charged CIS/ZnS QDs by using a basic solution of [-] MUA ligand where the thiol group aided in surface functionalization and the carboxylic group assisted in imparting the negative charge and dispersion in water.

Photoluminescence quenching experiments: In a typical experiment, a 3 mL aqueous solution of [+] CIS/ZnS QDs was prepared by optimizing the optical density at the

excitation wavelength (450nm) to be ~ 0.12 , corresponding to a concentration of $\sim 0.7 \mu\text{M}$.³ With the QDs acting as donors, aliquots of acceptor dye molecules were sequentially added to the QD solution and the solution was purged with Ar for 15 minutes after each addition. Spectral changes were monitored, both in terms of absorbance and steady-state photoluminescence. Correspondingly, time-resolved measurements via Time-Correlated Single Photon Counting (TCSPC) system were carried out using 459 nm laser as the excitation source. The fluorescence decay curves were fitted with tri-exponential functions with minimum χ^2 value. Similar procedure was adopted for the temperature dependent studies where the sample was allowed to equilibrate for 3 min at the set temperature before the measurement with a tolerance range of 0.5 °C. Similarly, solvent polarity dependent studies were also carried out in H₂O and 1:1 v/v H₂O:CH₃CN mixture.

Stern-Volmer Analysis: The nature of PL quenching between the donor and acceptor was analyzed using the Stern-Volmer equation:⁴

$$\frac{I_0}{I} = 1 + K_{SV}[Q]$$

where I_0 and I are the donor PL intensities in the absence and presence of the acceptor, respectively.

[Q] is the quencher concentration (M).

K_{SV} is the Stern-Volmer constant (M⁻¹).

From the plot of I_0/I vs the quencher concentration, with the intercept as 1, K_{SV} can be obtained from the slope. The Stern-Volmer constant, K_{SV} , is given as:

$$K_{SV} = k_q \cdot \tau_0$$

Where k_q is the bimolecular quenching constant (M⁻¹s⁻¹).

τ_0 is the lifetime of the donor in the absence of acceptor (ns).

All the Stern-Volmer plots were constructed from a set of three experiments.

Calculation of rate and efficiency of electron transfer process:

The rate (k_{ET}) and efficiency (E) of the electron transfer from [+] CIS/ZnS QD (donor) to acceptor dye was calculated using the following expressions.⁵

$$k_{ET} = \frac{1}{\tau} - \frac{1}{\tau_0} \quad \text{And} \quad E = 1 - \frac{\tau}{\tau_0}$$

where τ , τ_0 are the average lifetime of CIS/ZnS QDs in the presence and absence of acceptor dye.

Calculation of spectral overlap integral:

The spectral overlap integral was estimated following the well-accepted equation,⁴ which takes into account the fluorescence and absorption properties of the donor and acceptor moieties, respectively.

$$J(\lambda) = \int_0^{\infty} F_D(\lambda) \epsilon_A(\lambda) \lambda^4 d\lambda \quad M^{-1} cm^{-1} nm^4$$

$J(\lambda)$ is the spectral overlap between the emission of donor and absorption of the acceptor, $F_D(\lambda)$ is the normalized fluorescence intensity of the donor at a particular wavelength (λ), ϵ_A is the molar extinction coefficient of the acceptor. This is the standard way of calculating spectral overlap and to check the suitability of a donor-acceptor for FRET studies.

Instrumentation and Techniques used:

UV-Vis absorption studies: The absorption studies were performed in Shimadzu UV-3600 Plus UV-Vis/NIR spectrophotometer in a quartz cuvette of path length 1 cm. The absorption was monitored over an entire range of 300 nm – 1000 nm.

Steady-state photoluminescence studies: The photoluminescence experiments were carried out in Flurolog-3 spectrofluorometer (HORIBA Scientific) with Xe- lamp as the excitation source. The sample was excited at a wavelength of 450 nm where the dye acceptor molecules (ICG and MB) had negligible absorption.

Time-resolved photoluminescence measurements: Time-resolved studies were performed by using Time-Correlated Single Photon Counting system (Horiba Jobin Yvon-IBH and Delta Flex HORIBA Scientific for temperature dependent lifetime studies). The experiments were carried out using a 459 nm Nano LED as the excitation source with a time-to-amplitude converter (TAC) range of 1000 ns for 10,000 counts. The decay curves were deconvoluted and fitted using DAS analysis software v.6.5.6. The average lifetime (τ_{avg}) was calculated using following equation.⁴

$$\frac{\alpha_1\tau_1^2 + \alpha_2\tau_2^2 + \alpha_3\tau_3^2}{\alpha_1\tau_1 + \alpha_2\tau_2 + \alpha_3\tau_3}$$

Where τ is the lifetime and α is the pre-exponential factor with subscripts 1, 2, and 3 representing various species.

Zeta potential measurements: Zeta potential (ζ) was used to characterize the surface charge on CIS/ZnS QDs. The measurements were carried out in Zetasizer Nano series, Nano-2590 (Malvern Instruments, U.K.) having a 655 nm laser. The zeta potential is measured in terms of the electrophoretic mobility (U_E) (the velocity with which the charged particles are attracted to the oppositely charged electrodes) and is calculated using Henry's equation:

$$U_E = \frac{2\varepsilon\zeta f(ka)}{3\eta}$$

Where ε is the dielectric constant of the medium.

ζ is the zeta potential (mV).

$f(k_a)$ is Henry's function (value from Smoluchowski's approximation).

η is the viscosity of the medium (Pa.s).

X-Ray Diffraction (XRD) measurements: X-ray diffraction patterns were performed on Bruker D8 Advanced X-Ray Diffractometer using Cu K $_{\alpha}$ ($\lambda = 1.54 \text{ \AA}$) rays. Samples for XRD analysis were prepared by drop casting the [+] CIS/ZnS QDs on a glass substrate

High Resolution Transmission Electron Microscopy (HRTEM): The sample was prepared by drop casting 10 μL of [+] CIS/ZnS QDs solution on a 400-mesh carbon coated copper TEM grid (Ted Pella, Inc.). The sample was allowed to dry under ambient conditions and was further dried under vacuum. The image was taken in TECNAI G2 F20 TWIN at 200 keV.

Thermal gravimetric analysis (TGA):

TGA was performed using a NETZSCH STA 449F1 TGA-DSC system. The routine TGA were done under N $_2$ gas flow (20 mL/min) (purge + protective), and samples were heated from RT to 550°C at 2 K/min.

Fourier-transform infrared spectroscopy (FTIR):

Fourier transform infrared spectroscopy (FTIR) studies in solid state using KBr disc were obtained using NICOLET 6700 FTIR spectrometer.

^1H NMR:

^1H -NMR studies of colloidal dispersion in deuterated chloroform and water were performed on Bruker 400 MHz NMR spectrometer.

Section 2: Characterization of charged CIS/ZnS QD:

FTIR studies of OAm capped CIS/ZnS QDs

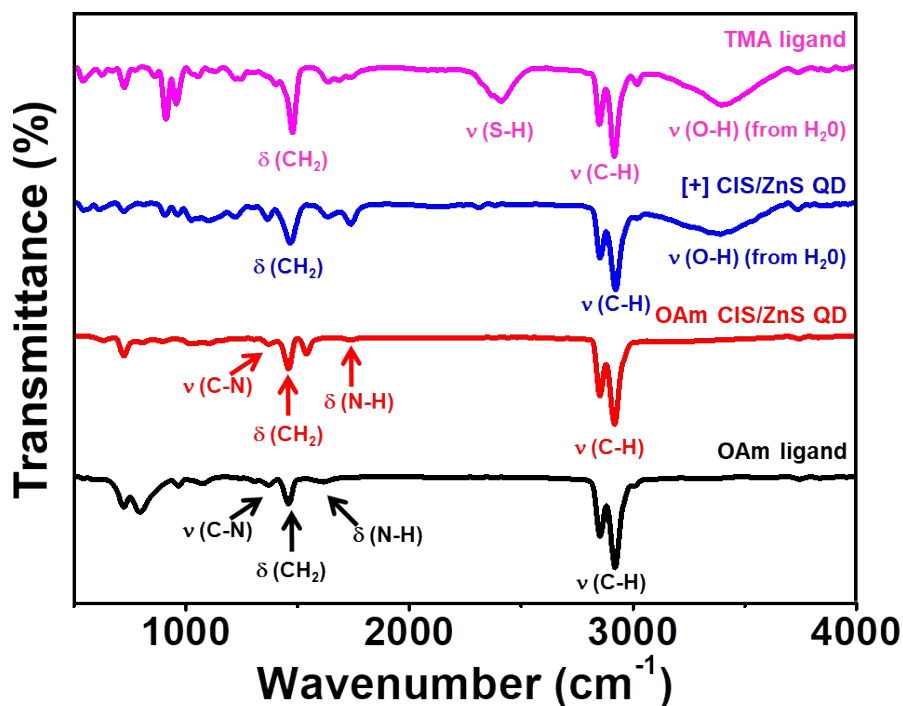


Fig. S1 FTIR spectra of Oleylamine (OAm) (black), OAm Capped CIS/ZnS QD (red), [+] CIS/ZnS QD (blue) and TMA ligand (magenta lane), along with the assignment of peaks.

FTIR studies of OAm capped CIS/ZnS QDs

The IR transmission bands observed for OAm and OAm capped CIS/ZnS QD samples are assigned in Table S1.

Table S1 Assignment of major IR peaks for OAm and OAm capped CIS/ZnS QD samples.

Samples	Major peaks observed	Peak assignments
OAm	2920 and 2853 cm^{-1}	-CH ₂ and -CH ₃ symmetric and asymmetric stretching vibrations ⁶
	~1616 cm^{-1}	N-H bending ⁶
	~1459 cm^{-1}	-CH ₂ bending ⁶
	~1372 cm^{-1}	C-N stretching ⁶
OAm capped	All the above mentioned	The N-H bending band was blue shifted to 1730 cm^{-1} , confirming the binding of OAm with the QD surface.

CIS/ZnS QD	characteristic peaks for OAm ligands were observed.	Similar blue shift has already been reported in other OAm capped QDs. ⁶
------------	---	--

The FTIR studies confirm the presence of OAm on the surface of OAm capped CIS/ZnS QDs.

FTIR studies of [+] CIS/ZnS QDs

The IR transmission bands observed for TMA and [+] CIS/ZnS QD samples are assigned in Table S2.

Table S2 Assignment of major IR peaks for TMA and [+] CIS/ZnS QD samples.

Samples	Major peaks observed	Peak assignments
TMA	2916 and 2850 cm ⁻¹	-CH ₂ and -CH ₃ symmetric and asymmetric stretching vibrations ⁶
	~2410 cm ⁻¹	S-H stretching ⁷
	~1477 cm ⁻¹	-CH ₂ bending ⁶
[+] CIS/ZnS QD	All the characteristic peaks for TMA ligand, except 2410 cm ⁻¹ peak, were observed	The absence of S-H stretching confirms that the TMA ligand is attached on the surface of CIS/ZnS QDs via the thiolate group. Similar absence of S-H stretching has already been reported in other thiol capped QDs. ⁷

The FTIR studies confirm the presence of TMA on the surface of [+] CIS/ZnS QDs.

The degree of functionalization of TMA (+) and OAm ligands on CIS/ZnS QDs was estimated using the combination of TGA and NMR experiments.

Thermal gravimetric analysis (TGA):

Calculation of the ligand coverage/degree of surface functionalization for QDs:

TGA experiments were performed by placing ~13 mg of QDs in the TGA pan and heating the QD sample in a nitrogen atmosphere at a rate of 2 °C/min up to 550 °C. The TGA plots obtained for OAm capped CIS/ZnS and [+] CIS/ZnS QDs are shown in Fig. S2.

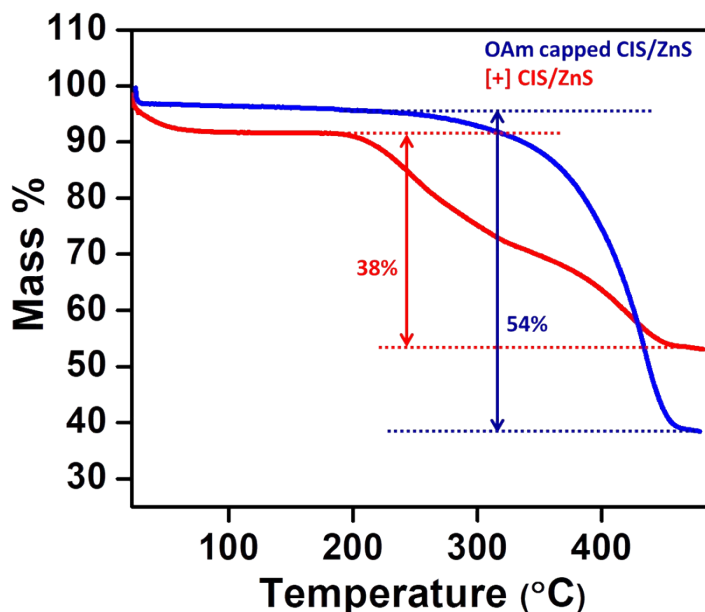


Fig. S2 TGA plots of OAm capped CIS/ZnS (blue) and [+] CIS/ZnS (red) QDs in the temperature range of 25 °C to 550 °C.

The nature of the TGA profile seen for TMA functionalized CIS/ZnS QD is similar to the reported TGA profile of TMA CdSe/ZnS QD.⁸

The concentration of OAm capped CIS/ZnS QD and [+] CIS/ZnS QD ($68.36 \mu\text{M}$ in 1 mL, 6.836×10^{-8} mol) were estimated from the position of first excitonic peak in the UV-Vis absorption spectrum and the QD size from TEM studies, as reported previously.³

The ligand coverage was estimated as per previous report.⁸

$$\text{Molar amount of ligand on QD surface} = \frac{\text{ligand weight}}{\text{molar mass of ligand}} \quad \text{-----} \quad (1)$$

$$\text{Number of ligands per QD} = \frac{\text{molar amount of ligand}}{\text{molar amount of QD}} \quad \text{-----} \quad (2)$$

$$\text{The ligand coverage} = \frac{\text{number of ligand per QD}}{\text{surface area of QD}} \quad \text{-----} \quad (3)$$

Surface area of QD = $4\pi r^2$ where, r is radius of the QD (The radius of CIS/ZnS QD was estimated to be 1.65 nm based on the TEM images)

According to the TGA data the weight loss for [+] CIS/ZnS QD was 38%, which is due to the decomposition of TMA ligands. From this loss, the weight of TMA ligand in [+] CIS/ZnS QD sample was estimated to be 4.94×10^{-3} g (the total weight of [+] CIS/ZnS QD sample

used for TGA experiment was 13.0×10^{-3} g). From equation (1), the molar amount of total ligand on QD surface was calculated to be 1.75×10^{-5} mol (molar mass of TMA is 281.5 g/mol). Finally, the number of TMA ligand per QD was determined to be 256 and the ligand coverage was determined to be 7.5 nm^{-2} using equations (2) and (3), respectively. Similar calculation was used to estimate the ligand coverage of OAm in OAm capped CIS/ZnS QD. The number of OAm ligand per QD was determined to be 384 and the ligand coverage was determined to be 11 nm^{-2} using equations (2) and (3), respectively.

Both FTIR and TGA studies revealed the presence of OAm and TMA ligands on the surface of OAm capped CIS/ZnS and [+] CIS/ZnS QDs, respectively. Further, the exclusivity of TMA ligands on [+] CIS/ZnS QD was confirmed using NMR studies.

Nuclear Magnetic Resonance (NMR) studies:

The ^1H NMR studies for OAm ligand was performed in deuterated chloroform (CDCl_3), and that of TMA ligand and [+] CIS/ZnS QD were performed in deuterated water (D_2O). The NMR spectra and peak assignments of various signals are shown in Fig. S3. The observation of the characteristic NMR signal for TMA ligand (~ 3.1 ppm, corresponding to the 9Hs of trimethyl groups on quaternary amine) in the QD sample confirms the presence of TMA ligand on the surface of [+] CIS/ZnS QDs. Similarly, the lack of any NMR signal in the range of 5-5.5 ppm (corresponding to the alkene protons of OAm) confirms the absence of any residual OAm on the surface of [+] CIS/ZnS QDs. Thus, it can be concluded that OAm was quantitatively replaced with TMA ligands during the place exchange reaction. It is worth mentioning that the NMR signals generally become broader for nanomaterial samples due to the inhomogeneity in the magnetic field.⁹

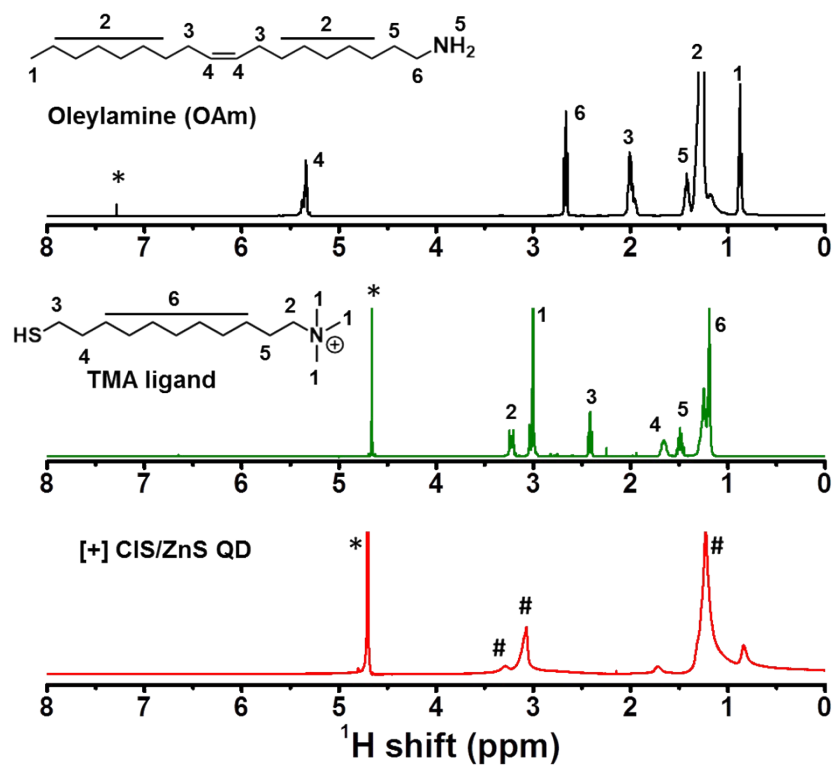


Fig. S3 ^1H NMR spectra of OAm, TMA and $[+]$ CIS/ZnS QD. Resonance peaks for solvent CDCl_3 and D_2O are labelled with *. The assigned of peaks in $[+]$ CIS/ZnS QD correspond to bound TMA ligands (labelled as #).

Steady-state and time-resolved studies of charged CIS/ZnS QDs:

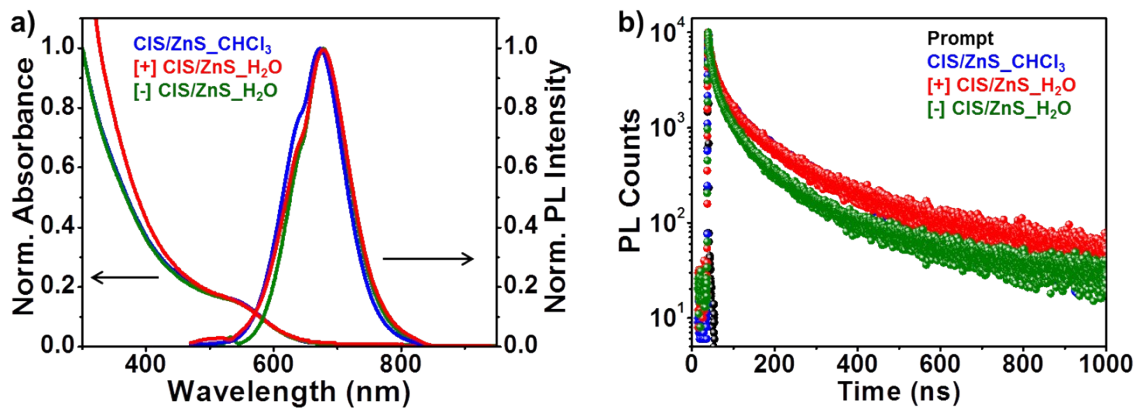


Fig. S4 (a) Normalized absorption and PL spectra of CIS/ZnS QDs before and after dispersion in water. (b) PL decay profiles of CIS/ZnS QDs before and after place exchange reaction, upon excitation with 459 nm laser.

Table S3 PL decay analysis of CIS/ZnS QD in a time window of 1 μs .

Sample	τ_1 (ns)	a_1	τ_2 (ns)	a_2	τ_3 (ns)	a_3	avg. τ (ns)	Chi. Sq
CIS/ZnS_CHCl ₃	6.6	0.58	43.4	0.31	192.2	0.11	121.60	1.13
[+] CIS/ZnS_H ₂ O	8.09	0.56	46.4	0.33	202.7	0.1	121.05	1.09
[-] CIS/ZnS_H ₂ O	5.6	0.62	33.1	0.31	147.6	0.07	78.29	1.15

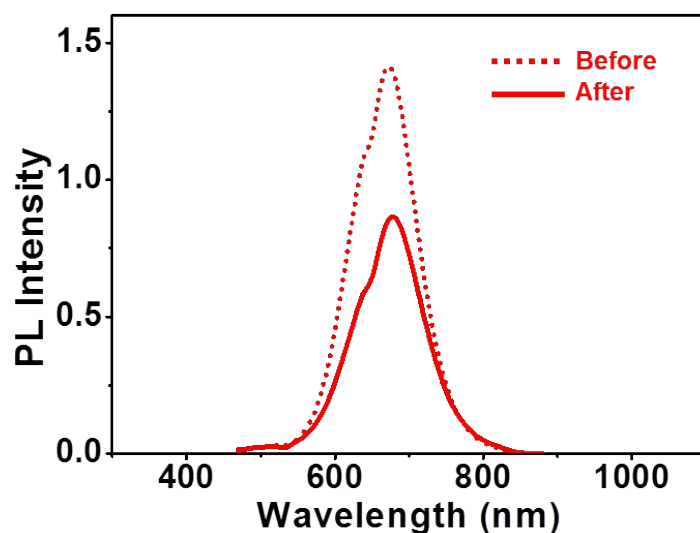


Fig. S5 Steady-state PL spectra of CIS/ZnS QD before and after the place exchange with [+] TMA ligands. Approximately 60% of the PL was retained in [+] CIS/ZnS QDs after the place exchange.

XRD analysis:

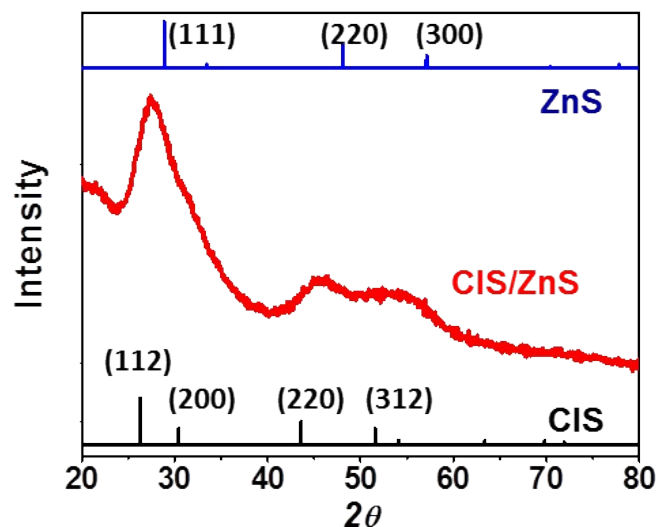


Fig. S6 Powder X-ray diffraction (XRD) patterns of [+] CIS/ZnS QD. Comparison of the XRD patterns of QD with bulk CIS and ZnS reference reveal chalcopyrite phase of [+] CIS/ZnS QD.¹⁰

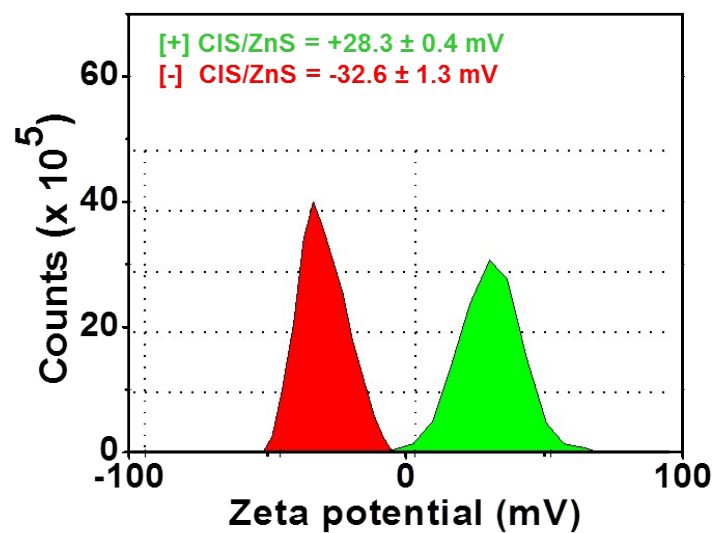


Fig. S7 Zeta potential (ζ) of [+] and [-] CIS/ZnS QDs confirming the charges on the surface of CIS/ZnS QDs. ζ of $+28.3 \pm 0.4$ mV and -32.6 ± 1.3 mV were observed for [+] and [-] CIS/ZnS QD, respectively. The error was estimated from three different measurements on three different samples.

Section 3: Photoinduced electron transfer studies:

[-] ICG Dye Properties:

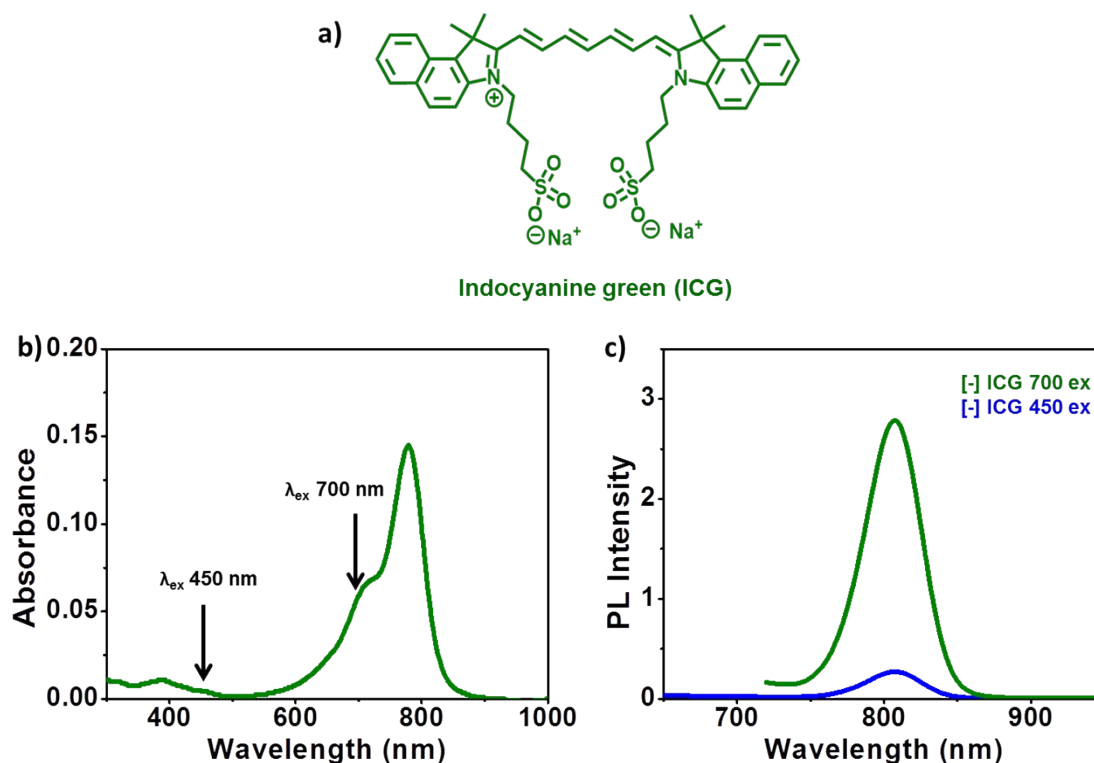


Fig. S8 (a) Chemical structure of Indocyanine green (ICG) dye. (b) Absorption and (c) PL spectra of [-] ICG dye in water. The PL spectra were recorded at 700 nm (green) and 450 nm (blue) excitation.

Energy/band level calculations of ICG and CIS/ZnS QD

The HOMO-LUMO energy levels of ICG dye were estimated from a combination of electrochemical and electronic absorption studies. Only one peak was observed in the cyclic voltammogram of ICG dye corresponding to the reduction process ($E_{pc} \sim -0.56$ V vs SHE; Fig. S9), which revealed the position of the LUMO to be -3.95 eV vs vacuum. The position of HOMO was estimated from offset of the band gap energy (~ 886 nm or 1.4 eV vs vacuum) obtained from our absorption studies. Accordingly, the position of HOMO of ICG dye was estimated to be -5.35 eV vs vacuum. We failed to perform cyclic voltammetry of [+] ICS/ZnS QD due to the instability of the QDs in the supporting electrolyte (tetra-butyl ammonium perchlorate). Hence, the conduction band position of CIS/ZnS QD was taken as -3.55 eV vs

vacuum from literature report.¹¹ The position of valence band was estimated from the knowledge on the offset of band gap obtained from our absorption studies (~ 685 nm or ~ 1.81 eV vs vacuum). Accordingly, the position of valence band of CIS/ZnS QD was estimated to be -5.36 eV vs vacuum. The energy levels estimated for CIS/ZnS QD and ICG dye are in good agreement with the literature reports.¹¹⁻¹³ Based on the above estimations, we have drawn the energy level diagram which is shown in **Fig. 2** in the main text.

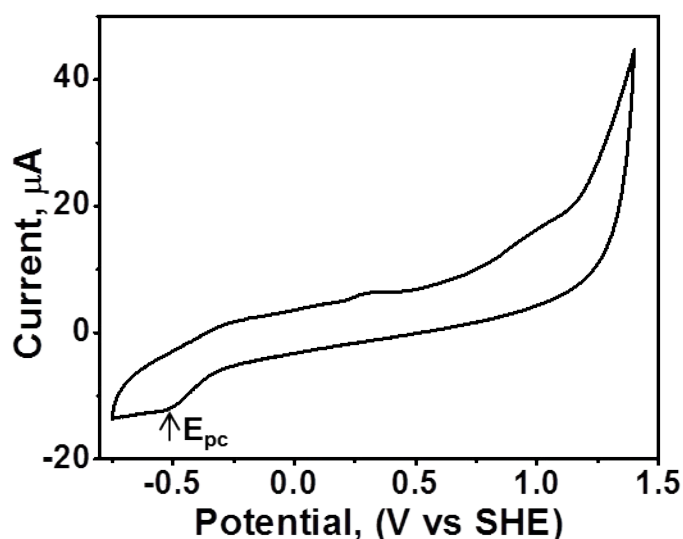


Fig. S9. Cyclic voltammogram of ICG dispersed in 50 mM tetra-butyl ammonium perchlorate (TBAP) solution in water, recorded at a scan rate of 50 mV/s

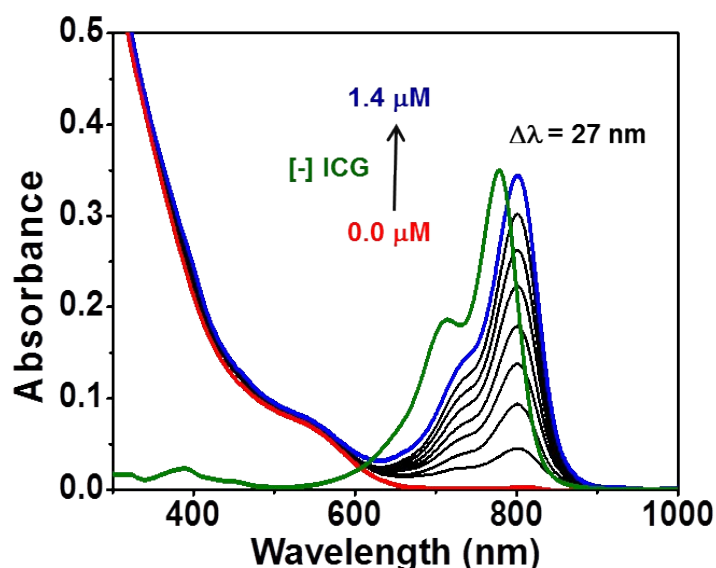


Fig. S10 Absorption spectral changes of [+] CIS/ZnS QD with increasing concentration of [-] ICG dye. The absorption spectrum of a separate solution of $1.4 \mu\text{M}$ [-] ICG is shown as the green curve. The absorbance of [-] ICG dye was red shifted by ~ 27 nm in [+] CIS/ZnS QD::[-] ICG dye complex confirming a strong ground state interaction between the QD and dye

[+] CIS/ZnS QD decay analysis in the presence of [-] ICG dye:

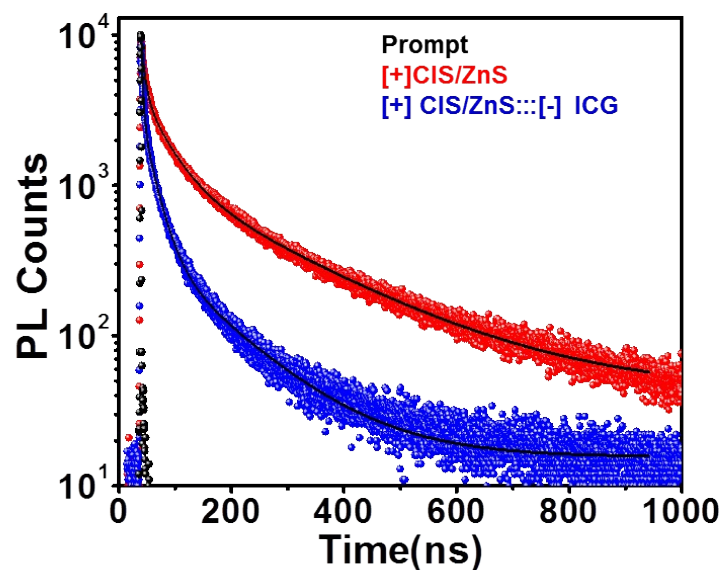


Fig. S11 PL decay profiles of [+] CIS/ZnS QD in the absence (red decay) and presence (blue decay) of 1.4 μM [-] ICG monitored at 655 nm, upon excitation with 459 nm laser source.

Table S4 PL decay analysis of [+] CIS/ZnS QD in the presence of [-] ICG dye measured in a time window of 1 μs .

Sample	τ_1 (ns)	a_1	τ_2 (ns)	a_2	τ_3 (ns)	a_3	avg. τ (ns)	Efficiency ^a
[+] CIS/ZnS_H ₂ O	8.09	0.56	46.4	0.33	202.7	0.1	121.05	0.70
[+] CIS/ZnS ::: [-] ICG_H ₂ O	3.69	0.72	20.1	0.25	93.6	0.03	35.61	

$${}^a\text{E} = 1 - \frac{\tau}{\tau_0}$$

Proof for Photoinduced electron transfer:

Experiment 1: Effect of solvent polarity on PL quenching studies

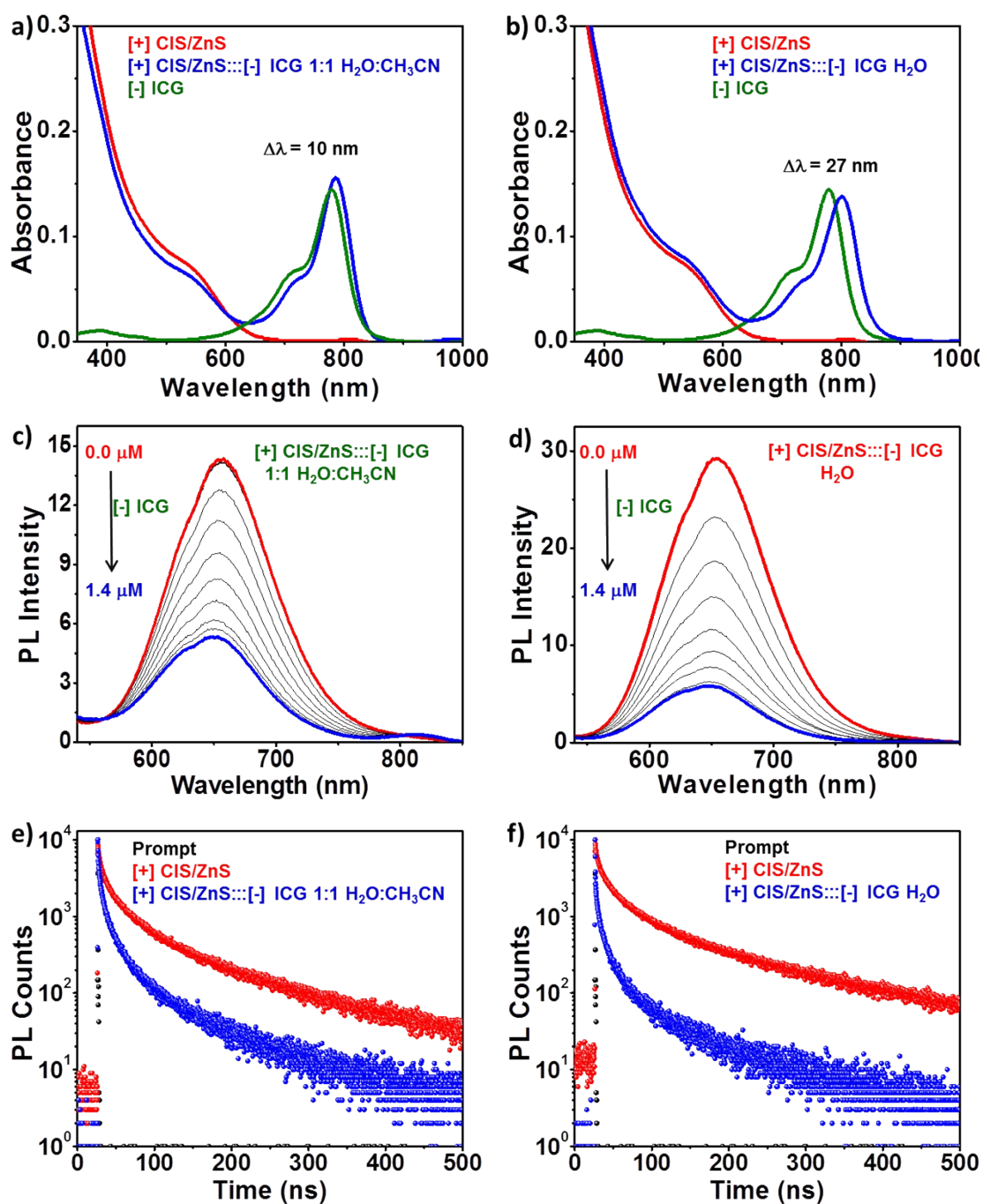


Fig. S12 Variation in the absorption of [+] CIS/ZnS QD upon addition of 1.4 μM [-] ICG dye in (a) 1:1 v/v H₂O: CH₃CN and (b) H₂O. The absorption spectrum of a separate solution of 1.4 μM [-] ICG is shown as the green curve. Steady-state PL spectral changes of [+] CIS/ZnS QD upon addition of 1.4 μM [-] ICG dye in (c) 1:1 v/v H₂O: CH₃CN and (d) H₂O. PL decay profiles of [+] CIS/ZnS QD in the absence (red decay) and presence (blue decay) of 1.4 μM [-] ICG in (e) 1:1 v/v H₂O: CH₃CN and (f) H₂O.

Experiment 2: Effect of temperature on photoluminescence quenching studies

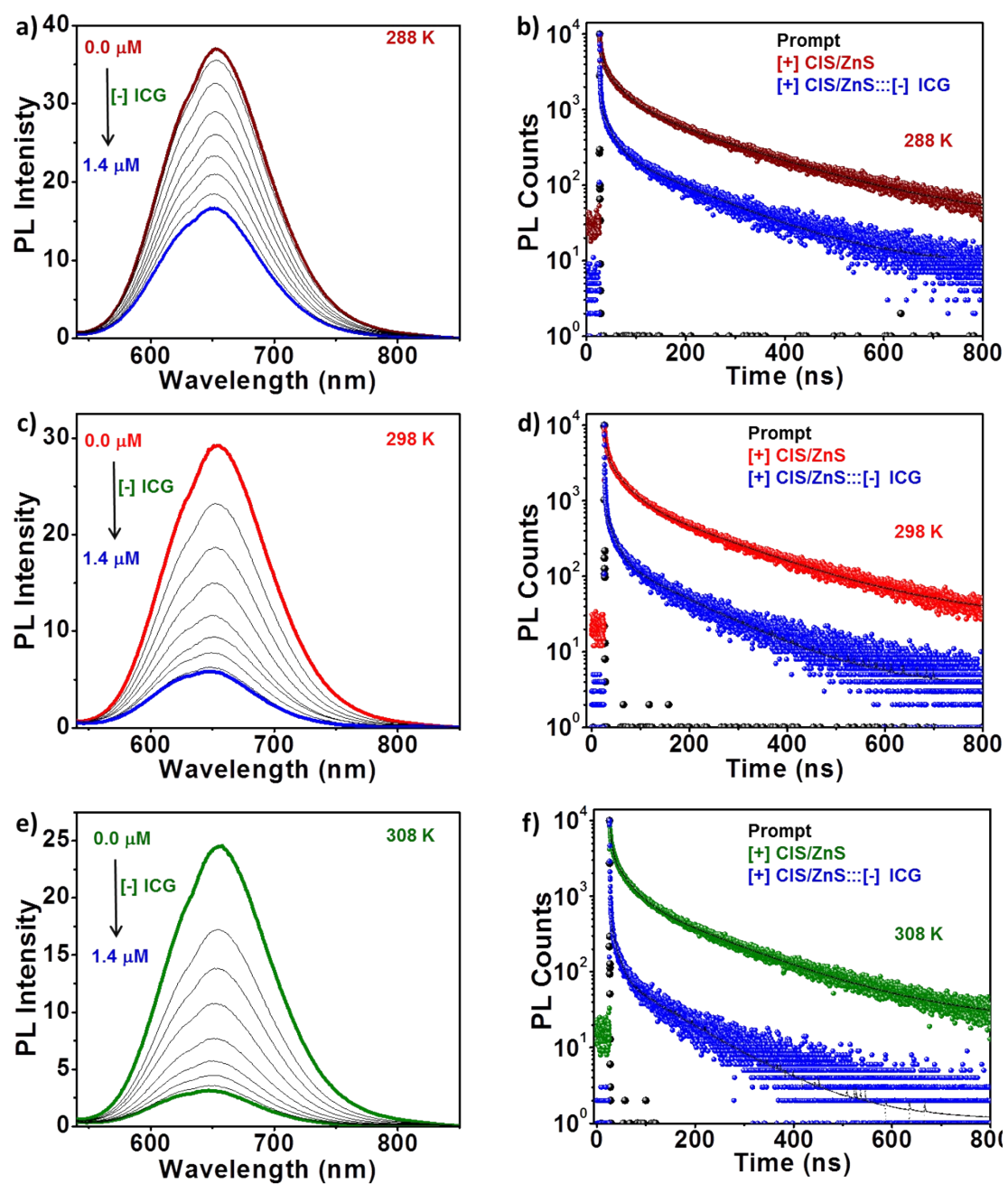


Fig. S13 Steady-state PL quenching of [+] CIS/ZnS QD by 1.4 μM [-] ICG dye at (a) 283 K, (c) 298 K and (e) 308 K. The corresponding PL lifetime quenching data are shown in (b), (d) and (f).

Table S5 Table summarizing various PL quenching and electron transfer parameters under different experimental conditions in [+] CIS/ZnS QD donor::[-] ICG dye acceptor nanohybrid.

[+] CIS/ZnS QD ::: [-] ICG dye complex	Solvent polarity		Temperature (K)		
	H ₂ O ($\epsilon \sim 78$)	1:1 H ₂ O:CH ₃ CN ($\epsilon \sim 47$)	283	298	308
PL quenching Efficiency ^a (Steady State)	80%	63%	60%	80%	89%
PL quenching Efficiency ^b (Lifetime)	70%	60%	48%	70%	78%
Stern-Volmer quenching constant ^c (k_{SV})	2.46×10^6 M ⁻¹	1.01×10^6 M ⁻¹	0.793×10^6 M ⁻¹	2.51×10^6 M ⁻¹	4.9×10^6 M ⁻¹
Bi-molecular quenching constant ^d (k_q)	2.18×10^{13} M ⁻¹ s ⁻¹	9.68×10^{12} M ⁻¹ s ⁻¹	5.9×10^{12} M ⁻¹ s ⁻¹	2.1×10^{13} M ⁻¹ s ⁻¹	4.76×10^{13} M ⁻¹ s ⁻¹
Rate of electron transfer ^e (k_{ET})	2.0×10^7 s ⁻¹	1.44×10^7 s ⁻¹	6.78×10^6 s ⁻¹	1.89×10^7 s ⁻¹	3.28×10^7 s ⁻¹

$${}^a E = 1 - \frac{I}{I_0}; \quad {}^b E = 1 - \frac{\tau}{\tau_0}; \quad {}^{c,d} K_{SV} = k_q \tau_0; \quad {}^e k_{ET} = \frac{1}{\tau} - \frac{1}{\tau_0}$$

Proof for electrostatically driven photoinduced electron transfer in [+] CIS/ZnS QD donor::[-] ICG dye acceptor nanohybrid.

Control experiment # 1: Breaking of [+] CIS/ZnS::[-] ICG dye Complex in the presence of phosphate (PO_4^{3-}) ion.

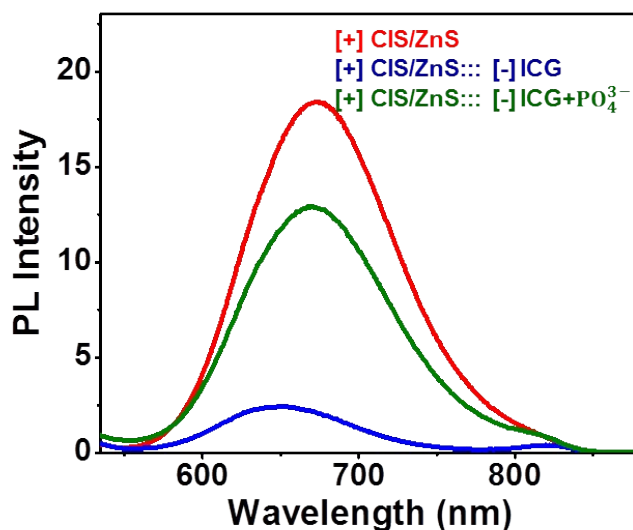


Fig. S14 PL spectral changes of [+] CIS/ZnS::[-] ICG dye complex upon the addition of 50 mM PO_4^{3-} ion. The recovery in the PL of [+] CIS/ZnS in the presence of PO_4^{3-} ion confirms the breaking of [+] CIS/ZnS::[-] ICG dye complex, as a result of screening of charges on QD and dye by PO_4^{3-} ions.

Control experiment # 2

Electron transfer studies between [-] CIS/ZnS QD and [+] MB dye:

Control experiments were carried out with [+] CIS/ZnS QD as a donor and [+] MB dye as an acceptor. The charges are same on the surface of donor and acceptor, which prevented the complex formation and the process of electron transfer.

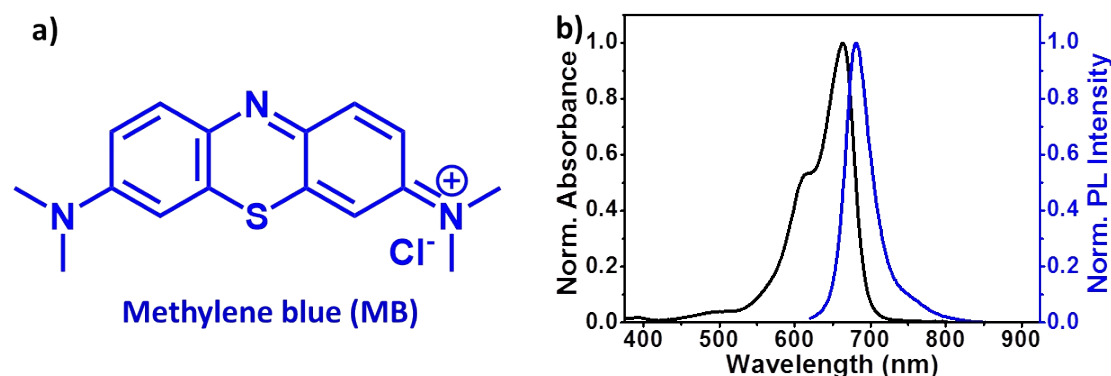


Fig. S15 (a) Chemical structure of methylene blue (MB) dye. (b) Normalized absorption (black spectrum) and PL (green spectrum) spectra of [+] MB dye in water.

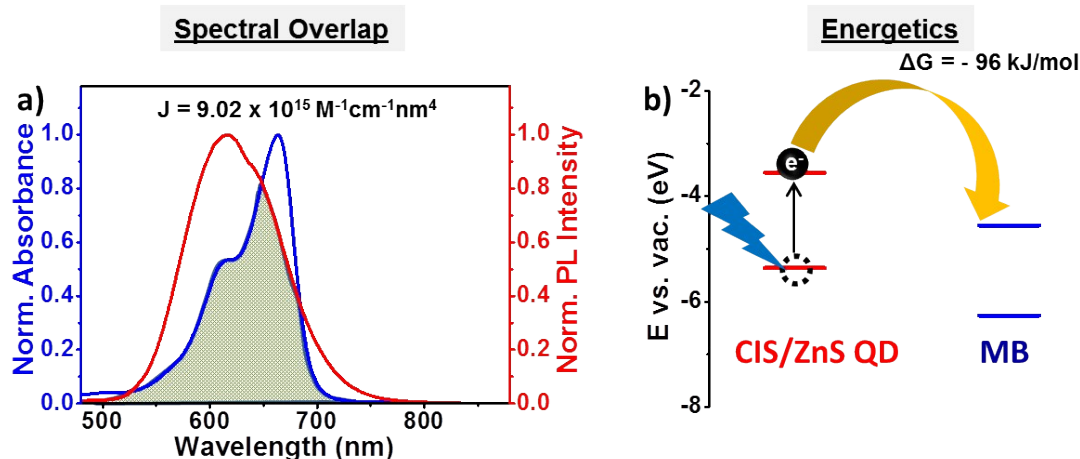


Fig. S16 (a) Spectral overlap between the PL of [+] CIS/ZnS QD and the absorption of [+] MB dye. (c) Energy levels of [+] CIS/ZnS QD and [+] MB dye, indicates an electron transfer process is thermodynamically feasible from the CIS/ZnS QDs to MB dye.

PL quenching studies in similarly charged [+] CIS/ZnS QD::: [+] MB dye nanohybrid

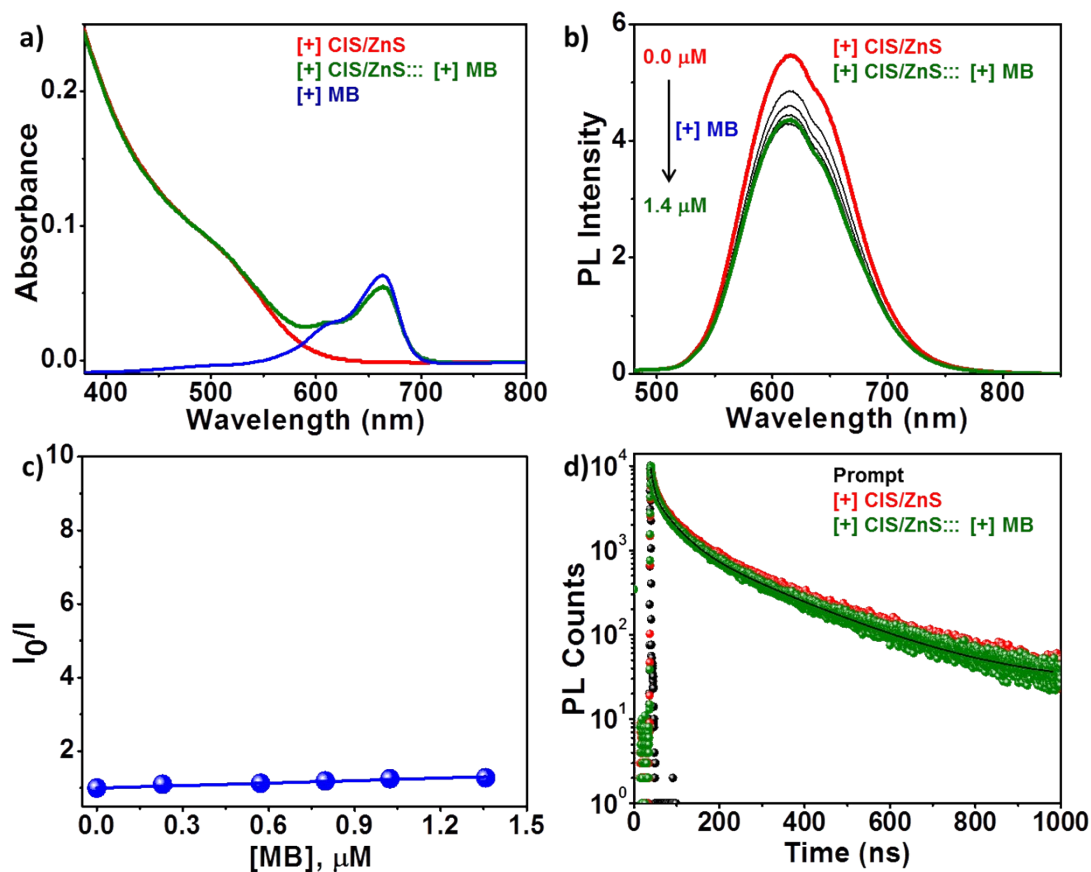
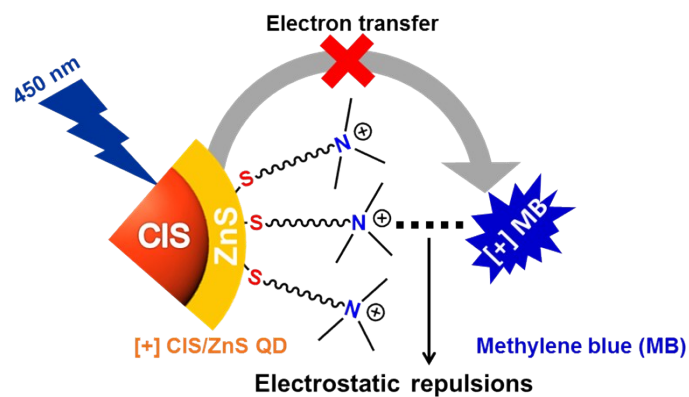


Fig. S17 (a) Absorption spectra of [+] MB dye in the absence and presence of [+] CIS/ZnS QD. (b) Spectral changes in the PL of [+] CIS/ZnS QD upon sequential addition of varying concentrations of [+] MB dye, and (c) the corresponding Stern-Volmer plot. (d) PL decay profiles of [+] CIS/ZnS QDs in the absence and presence of 1.4 μM [+] MB dye, collected at the donor emission of 618 nm.



Scheme S1: Schematic representation of [+] CIS/ZnS QD and [+] MB dye in water.

Table S6 PL decay analysis of [+] CIS/ZnS QD in the presence of [+] MB dye measured in a time window of 1 μ s.

	τ_1 (ns)	a_1	τ_2 (ns)	a_2	τ_3 (ns)	a_3	avg τ (ns)
[+] CIS/ZnS_H ₂ O	7.549	0.52	48.26	0.33	200.79	0.15	136.99
[+] CIS/ZnS::[+] MB_H ₂ O	6.544	0.54	44.48	0.33	193.95	0.13	128.17

PL quenching studies in oppositely charged [-] CIS/ZnS QD::: [+] MB dye nanohybrid

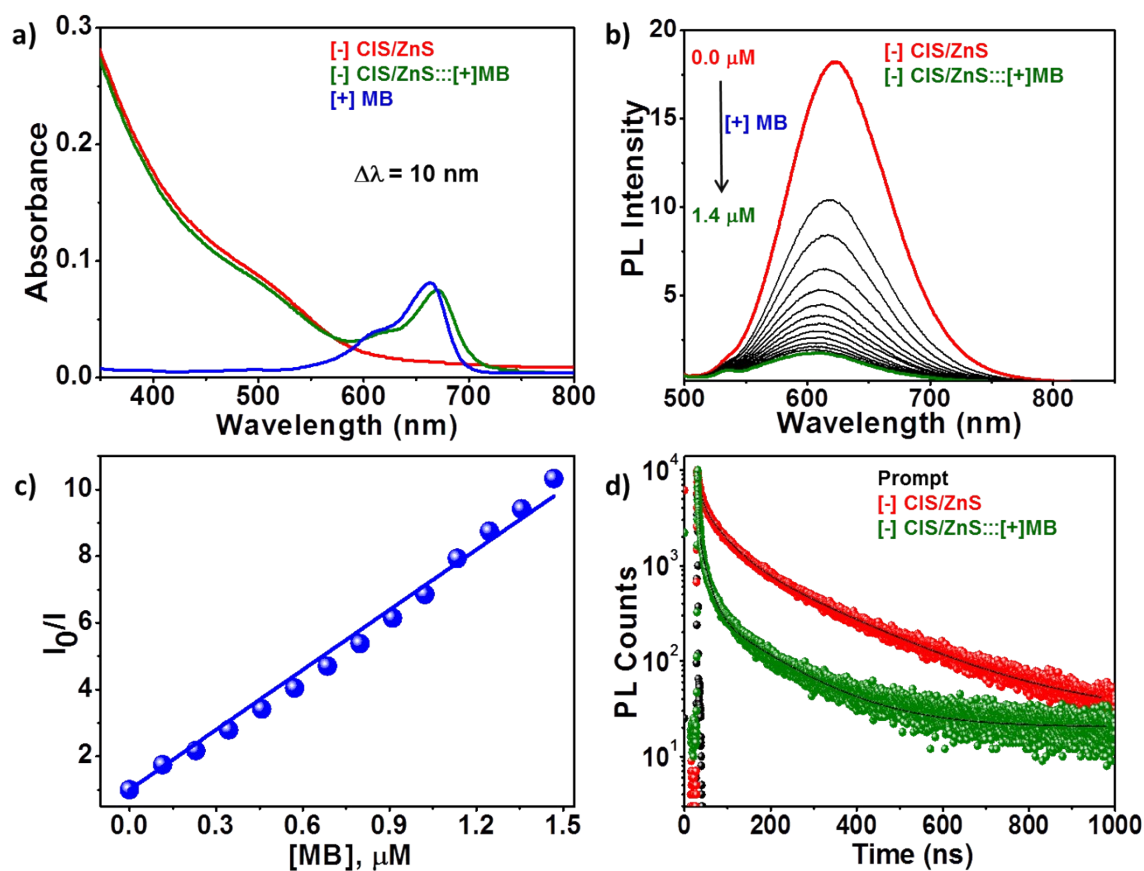


Fig. S18 (a) Absorption spectra of [+] MB dye in the absence and presence of [-] CIS/ZnS QDs. (b) Spectral changes in the PL of [-] CIS QDs upon sequential addition of [+] MB dye, and (c) the corresponding Stern-Volmer plot. (d) PL decay profiles of [-] CIS/ZnS QD in the absence and presence of 1.4 μM [+] MB dye, collected at the donor emission of 622 nm.

Table S7 PL decay analysis of [-] CIS/ZnS QD in the presence of [+] MB dye measured in a time window of 1 μs.

	τ_1 (ns)	a_1	τ_2 (ns)	a_2	τ_3 (ns)	a_3	avg τ (ns)	efficiency ^a
[-] CIS/ZnS_H ₂ O	7.464	0.60	39.23	0.32	163.9	0.08	88.73	0.65
[-] CIS/ZnS:::[+] MB_H ₂ O	2.07	0.85	17.88	0.13	81.58	0.02	31.19	

$${}^a E = 1 - \frac{\tau}{\tau_0}$$

References:

1. J. Tien, A. Terfort and G. M. Whitesides, *Langmuir* 1997, **13**, 5349–5355.
2. a) D. Deng, Y. Chen, J. Cao, J. Tian, Z. Qian, S. Achilefu, Y. Gu, *Chem. Mater.* 2012, **24**, 3029–3037.
3. M. Booth, A. P. Brown, S. D. Evans and K. Critchley, *Chem. Mater.*, 2012, **24**, 2064–2070.
4. J. R. Lakowicz, *Principles of Fluorescence Spectroscopy*, 3rd ed., Springer: New York, **1999**.
5. A. Kongkanand, K. Tvrđy, K. Takechi, M. Kuno and P. V. Kamat, *J. Am. Chem. Soc.*, 2008, **130**, 4007–4015.
6. X. Lu, H. -Y. Tuan, J. Chen, Z. Li, B. A. Korgel and Y. Xia, *J. Am. Chem. Soc.*, 2007, **129**, 1733–1742.
7. E. Raphael, D. H. Jara and M. A. Schiavon, *RSC Adv.*, 2017, **7**, 6492–6500.
8. Y. C. Yeh, K. Saha, B. Yan, O. R. Miranda, X. Yu and V. M. Rotello, *Nanoscale*, 2013, **5**, 12140–12143.
9. A. Badia, W. Gao, S. Singh, L. Demers, L. Cuccia and L. Reven, *Langmuir*, 1996, **12**, 1262–1269.
10. E. Raphael, D. H. Jara and M. A. Schiavon, *RSC Adv.*, 2017, **7**, 6492–6500.
11. P. K. Santra, P. V. Nair, K. George Thomas and P. V. Kamat, *J. Phys. Chem. Lett.*, 2013, **4**, 722–729.
12. T.-L. Li, Y.-L. Lee and H. Teng, *J. Mater. Chem.*, 2011, **21**, 5089.
13. T. C. Barros, S. H. Toma, H. E. Toma, E. L. Bastos and M. S. Baptista, *J. Phys. Org. Chem.*, 2010, **23**, 893–903